unknown; only in situ measurements which have minimal effects on the local flow can yield this information.

IV. Summary

In any characterization of the performance of an engine such as the secondary combustor of an air-augmented rocket, a combustion efficiency is defined as the experimentally determined change in some parameter (e.g., temperature) divided by its theoretically calculated value. One contributing factor to discrepancies in efficiency can arise in calculation of this latter value, because the composition of the fuel, specifically its particulate components, is frequently unknown. In the present study it has been demonstrated that these particles can contain $NH_4B_5O_8 \cdot 4H_2O$, NH_4Cl, C, and other organics in addition to B and B_2O_3. Clearly, before the performance of a motor is compared with theory, tests similar to those reported here must be conducted to determine the input for the analytical calculation.

Size analyses of the particles collected in the present investigation have also been discussed. The as-received B has a mode on the order of 0.25 μ, and electron micrograph studies of the particles collected from the primary motor exhaust suggest that no significant change in this mode has occurred. However, since the influence of the experimental collection method on the measured particle size distribution is unknown, this conclusion cannot be stated unequivocally.

References

[1] Schadow, K., "Experimental Investigation of Boron Combustion in Air-Augmented Rockets," *AIAA Journal*, Vol. 7, No. 10, Oct. 1969, pp. 1870–1876.

[2] Sargent, W. H., Anderson, R. S., and Duvvuri, T., "Investigation of Air-Augmented Rocket Combustion and Mixing Processes," AFRPL-TR-67-271, Oct. 1967, Air Force Rocket Propulsion Lab., Edwards Air Force Base, Calif.

[3] Mellor, A. M. and Gouldin, F. C., "Study of the Particulate Matter in the Exhaust of a Boron-Loaded Solid Propellant," USAMICOM RK-TR-70-11, Aug. 1970.

[4] Goede, P. J. and Skifstad, J. G., "Rate Processes in the Secondary Combustion of an Air-Augmented Solid Propellant," AIAA Paper 70-734, New York, 1970.

[5] Allen, T., *Particle Size Measurement*, Chapman and Hall, London, 1968.

[6] Gardner, W. E., private communication, Oct. 1969, Sloan Research Industries, Santa Barbara, Calif.

[7] Gardner, W. E., private communication, Dec. 1969, Sloan Research Industries, Santa Barbara, Calif.

[8] Shelnutt, J. W., private communication, Jan. 1970, Aerospace Research Labs., Wright-Patterson Air Force Base, Dayton, Ohio.

OCTOBER 1971 AIAA JOURNAL VOL. 9, NO. 10

Magnetohydrodynamic Instabilities in a Weakly Ionized, Radiating Plasma

MERRITT L. HOUGEN* AND JAMES E. MCCUNE†
Massachusetts Institute of Technology, Cambridge, Mass.

A unified, linear theory is formulated for MHD waves at low magnetic Reynolds number, propagating transverse to the magnetic field in a weakly ionized, radiating plasma. The set of equations obtained from a two-fluid model yields a fifth-order dispersion relation whose roots correspond to four waves: magnetoacoustic (a paired wave), thermal, electrothermal, and "ionization-rate." To bring out the physics of each of these waves, simplifying assumptions are made, and "simple" analytical wave solutions are found. By taking advantage of the wide separation of the roots in the complex plane, "distinct" wave solutions are obtained in which many limitations of the "simple" wave solutions are absent and which are in excellent agreement with the roots of the full dispersion relation, obtained numerically. Both thermal and magnetoacoustic waves are shown to require a two-fluid model for proper description. In particular, the latter mode requires the inclusion of the rate of change of electron enthalpy for wavelengths $\lesssim$ 0.1 m, at typical MHD generator conditions. The electrothermal wave instability region is much larger than previously thought, whereas the "ionization rate wave" is always stable.

Nomenclature

a_0 = steady-state speed of sound
$\mathbf{B}$ = magnetic field
B_{00} = Planck function at line center
C_{en0}, C_{ei0} = steady-state collisional loss
C_r = C_{ei0}/C_{en0}
d = width of MHD channel
D/Dt = $(\partial/\partial t) + \mathbf{u}_g \cdot \nabla$
e = elementary charge ($e = 1.60210 \times 10^{-19}$ coul)
e_* = internal molecular energy per unit mass
$\mathbf{E}$ = electric field measured in laboratory frame
$\mathbf{E}'$ = electric field measured moving at the heavy-gas velocity
h = Planck's constant ($h = 6.624 \times 10^{-34}$ joule-sec)
H = $\lambda_0 T_{e0} k^2/(1 + \beta_0^2)$, electronic heat conduction loss as function of wave number
I = $J_0 B_0/k p_{g0}$, interaction number

Received June 10, 1970; revision received January 15, 1971. This work was carried out within the Research Laboratory of Electronics of Massachusetts Institute of Technology, supported by the Air Force Aero Propulsion Laboratory, Contract F33615-67-C-1148, and was part of a Ph.D. dissertation submitted by M. L. Hougen to M.I.T. The authors are pleased to acknowledge fruitful discussions with J. L. Kerrebrock, G. Bekefi, and A. Solbès.

Index categories: Electric Power Generation Research; Plasma Dynamics and MHD.

* Research Assistant, Department of Aeronautics and Astronautics; presently student, Stanford University School of Medicine, Stanford, Calif.

† Professor, Department of Aeronautics and Astronautics.

$\mathbf{J}$ = current density
K = Boltzman constant ($K = 1.38054 \times 10^{-23}$ joule/°K)
$\mathbf{k}, k$ = wave number or propagation vector, $k \equiv |\mathbf{k}|$
k_b = recombination rate coefficient
K_n = equilibrium constant
m = mass
m_{00} = optical depth per unit length at line center
n = number density
p = pressure
r = $\partial(\ln n_e)/\partial(\ln T_e)_{k_b=\infty}$
R = radiation loss
R_{em} = $\mu_0\sigma_0 uL$, magnetic Reynolds number
t = time
T = temperature
T_R = T_{e0}/T_{g0}
$\mathbf{u}$ = velocity
u_{eC} = electron drift velocity
$\langle v_{e0}\rangle$ = average electron thermal speed
x = direction coordinate
β = Hall parameter
γ = ratio of specific heats
δ = collisional loss parameter
$\Delta\nu$ = frequency half-width
ϵ_i = ionization energy of alkali atom
ϵ_0 = permittivity in a vacuum
ϵ_{e0} = $\frac{3}{2}KT_{e0}$
θ = angle from $\mathbf{k}$ to $\mathbf{J}_0$
λ = $K^2T_e n_e/m_e\bar{\nu}$, electronic heat conduction coefficient ($\bar{\nu}$ from Ref. 15)
λ = perturbation wavelength
Λ = $12\pi(\epsilon_0 K/e^2)^{3/2}(T_e^{3/2}/n_e^{1/2})$
μ_0 = permeability in a vacuum
ν = collision frequency for momentum transfer
ν_0 = radiation frequency at line center
ρ = mass density
ρ_c = plasma charge density
σ = electrical conductivity
ϕ = steady-state ratio of radiation loss to neutral collisional loss
ω = angular frequency in laboratory coordinates
ω' = Doppler shifted frequency

Subscripts

a = alkali atom
b = buffer atom
e = electron
g = heavy gas
i = imaginary component
n = neutral
0 = steady-state value
r = real component
t = total

Introduction

MAGNETOHYDRODYNAMIC generators, operating in a closed cycle at high gas pressure (1–10 atm) and employing slightly ionized, seeded plasmas, must run in a nonequilibrium mode to obtain sufficient electrical conductivity. Although the ideal theory predicts sufficient electron temperature elevation to obtain a high conductivity, this conductivity has not been reached in experiments run in generator configurations. Several phenomena such as gas turbulence, circulating currents due to the Hall effect, boundary-layer shorting, and electrode losses contribute to this failure; but in many cases much of the difficulty may be due to unstable MHD waves with which this paper is concerned.

"Magnetoacoustic waves" were first discussed by Herlofson[1] for very high magnetic Reynolds numbers. More recently, Velikhov[2] showed that, for a *small* magnetic Reynolds number in a *weakly* ionized plasma, acoustic waves in a magnetic field could be influenced (and destabilized) by fluctuations of the Hall parameter. Both of these types of disturbance have been shown to be limits of the same mode,[3] the "magnetoacoustic" wave. McCune[4] further discussed the work of Velikhov and extended it to include the important fluctuations in the conductivity. Both Fishman[5] and McCune[6] indicate that the magnetoacoustic instability can be controlled by external circuitry. Fishman's work extends in an essential way the earlier analyses of Locke and McCune[7] and Powers and Dicks,[8] which, although they include the effects of steady-state gradients, do not include boundary conditions and coupling to external circuitry. Messerle[9] has discussed unstable magnetoacoustic waves in an MHD induction generator.

All of the foregoing analyses employ a one-fluid MHD model of the plasma. Hollweg[10] was the first to employ fairly complete two-fluid equations in this context and to discuss the effects on magnetoacoustic waves of an elevated electron temperature. Eliseev[11] has discussed the effects of the direction of wave propagation.

Another type of MHD wave is the so-called "thermal" wave. Wright,[12] using both one- and two-fluid models and assuming incompressibility and no Hall effect, analyzed waves parallel to the steady-state current. This wave is simply the "thermal wave" of ordinary heat conduction with the effects of Joule heating added. With the addition of Joule heating, an instability can occur. Powers and Dicks[8] expanded the treatment of Wright by including steady-state gradients. However, only a one-fluid model was used, and heat conduction was neglected. Edwards,[3] although he did not identify it as such, also obtained the "thermal" wave (viz., his "parameter variation" wave).

Electrothermal waves, first treated by Kerrebrock[13] and by Velikhov and Dykhne[14] independently and at about the same time, are substantially different from the foregoing magnetoacoustic and thermal waves: here, oscillations of the electron temperature and of the electron density can occur almost independently of the heavy gas, caused by perturbations of the electron density gradient and of the electric field. In the original analyses, the heavy gas was assumed not to fluctuate at all; this assumption is relaxed in the present study. Recently Nelson and Haines[15] have solved numerically an essentially complete second-order dispersion relation for the electrothermal and "ionization rate" modes (see following sections). Motion of the heavy gas and the steady-state radiation loss were neglected in that work.‡ Solbès[16] and Zampaglione,[17] in obtaining stability criteria, have included a component of the steady-state current parallel to the magnetic field. Smith[18] has analyzed the effect of a large electron density gradient.

In addition to the theoretical treatments mentioned previously, many experiments,[19–26] run at MHD generator conditions, indicate the presence of MHD instabilities. For this reason, from an engineering standpoint, it is very important to have a fuller understanding of MHD waves than the foregoing limited analyses have provided. For example, at the outset of the present study it was not clear what the interrelationships of the waves might be and what effect this might have on their relative importance. It is the intention of this paper to help clarify this and other points by providing a more general theory of MHD waves travelling perpendicular to the magnetic field at low magnetic Reynolds number. This more general theory includes the effects of radiation, a finite recombination rate, Coulomb collisions, an elevated electron temperature, and heat conduction; it also includes both the previous limiting cases of the waves and any (linear) interactions between the modes.

To complete this task, the order of procedure is as follows: a set of equations based on a two-fluid model and consisting

‡ Since completion of this manuscript, the authors became aware of an extension of Ref. 15 by A. H. Nelson: "Wave Propagation and Instabilities in a Magnetized, Partially Ionized Gas Under Non-Equilibrium Conditions," Ph.D. Thesis, Imperial College, London (October, 1969). Here Nelson also studies magnetoacoustic waves, and in addition has analyzed the effect of boundary conditions and external circuitry on electrothermal waves.

of moments of the Boltzmann equation, together with Maxwell's equations, is presented. These equations are linearized according to first-order perturbation theory and then analyzed assuming plane wave perturbations. The explicit effect of radiation is included, taking advantage of the results of Lutz.[27] Following this, assumptions are imposed upon the general wave equations which lead analytically to the various limiting cases of the waves previously identified, as discussed previously. The full equations of a low magnetic Reynolds number plasma are shown to yield a general (fifth-order) dispersion relation; this has been solved on a computer. If one takes advantage of the generally wide spacing of the locations of the resulting roots in the complex frequency plane, results for "distinct" waves without limiting (physical) assumptions can also be given. These, along with the "simple" wave theories, are compared with the exact computer solutions. Finally, by comparison with accumulated experimental data, the applicability of the general theory is discussed.

General MHD Equations

The working fluid of the MHD generator is a slightly ionized, seeded plasma, consisting of a noble "buffer" gas and an alkali metal vapor "seed" gas. The theoretical model assumes two fluids, the electron gas and the heavy gas, the latter being composed of the alkali ions, alkali atoms, and buffer atoms. The assumptions at this point are that the buffer gas is negligibly ionized, that there is no "ion slip," and that the positive ions and neutral molecules are at the same temperature. This two-fluid model requires six scalar equations: two continuity equations, two energy equations, and the two scalar Maxwell equations; and four vector equations: two momentum equations and the remaining two Maxwell equations.

Heavy-Gas Equations

Continuity:

$$(D\hat{n}_g/Dt) + \hat{n}_g\nabla\cdot\hat{\mathbf{u}}_g = 0 \tag{1}$$

where the caret denotes total quantity. The source term on the right-hand side has been neglected because of the low degree of ionization ($\hat{n}_e \ll \hat{n}_g$).

Momentum:

$$\hat{\rho}_g(D\hat{\mathbf{u}}_g/Dt) = -\nabla\hat{p}_g + \hat{\mathbf{J}} \times \hat{\mathbf{B}} \tag{2}$$

where the heavy-gas viscosity has been neglected, and the MHD (quasi-neutrality) assumption has been made.

Energy:

$$\hat{\rho}_g\left(\frac{D\hat{e}_g}{Dt} + \hat{p}_g\frac{D(\hat{\rho}_g)^{-1}}{Dt}\right) = \hat{n}_e m_e\left(\frac{\delta_a\hat{\nu}_{ea}}{m_a} + \frac{\delta_b\hat{\nu}_{eb}}{m_b}\right)\times$$
$$\frac{3}{2}K(\hat{T}_e - \hat{T}_g) + \left(\frac{m_e^{1/2}e^4}{(2\pi)^{3/2}K^{1/2}\epsilon_0^2}\right)\frac{\hat{n}_e^2\ln\Lambda}{m_a\hat{T}_e^{3/2}}(\hat{T}_e - \hat{T}_g) \tag{3}$$

where the collisional loss parameters[13] δ_a and δ_b include the effect of nonelectronic degrees of freedom only. Assuming a detailed balance for excitation and photo-de-excitation, radiation and electronic degrees of freedom do not affect the heavy gas. Defining $\hat{T}_e$ in the sense used here requires a near-Maxwellian electron distribution[28] ($n_{e0} \geq 10^{13}$ cm^{-3}). Heavy-gas heat conduction and viscosity are assumed negligible ($\lambda \geq 1$ mm for typical MHD generator conditions).[29]

Electron-Gas Equations

Continuity:

$$(D\hat{n}_e/Dt) + \hat{n}_e\nabla\cdot\hat{\mathbf{u}}_g - e^{-1}\nabla\cdot\hat{\mathbf{J}} = \hat{k}_b(\hat{K}_n\hat{n}_e\hat{n}_a - \hat{n}_e^3) \tag{4}$$

where the valence electrons and bound electrons are assumed to be in equilibrium ($n_{e0} \geq 10^{13}$ cm^{-3}),[28] and the ionization and recombination process $e^- + a \rightleftarrows e^- + e^- + a^+$ is assumed dominant ($T_{e0} \geq 1500°$K).[10]

Momentum:

$$\hat{\mathbf{J}} = \hat{\sigma}[(\hat{\mathbf{E}}' + (e\hat{n}_e)^{-1}\nabla\hat{p}_e - (e\hat{n}_e)^{-1}\hat{\mathbf{J}} \times \hat{\mathbf{B}}]) \tag{5}$$

where electron viscosity and inertia have been neglected.

Energy:

$$\frac{D}{Dt}\left[\left(\frac{3}{2}K\hat{T}_e + \epsilon_i\right)\hat{n}_e\right] + \left(\frac{3}{2}K\hat{T}_e + \epsilon_i\right)\hat{n}_e\nabla\cdot\hat{\mathbf{u}}_g +$$
$$\hat{p}_e\nabla\cdot\hat{\mathbf{u}}_g = \hat{\lambda}\nabla\cdot\mathbf{M}\nabla\hat{T}_e + e^{-1}\nabla\cdot\left(\frac{5}{2}K\hat{T}_e + \epsilon_i\right)\hat{\mathbf{J}} + \hat{\mathbf{J}}\cdot\hat{\mathbf{E}}' -$$
$$\hat{n}_e m_e\left(\frac{\delta_a\hat{n}_a\hat{\nu}_{ea}}{m_a} + \frac{\delta_b\hat{n}_b\hat{\nu}_{eb}}{m_b}\right)\frac{3}{2}K(\hat{T}_e - \hat{T}_g) -$$
$$\left(\frac{m_e^{1/2}e^4}{(2\pi)^{3/2}K^{1/2}\epsilon_0^2}\right)\frac{\hat{n}_e\ln\hat{\Lambda}}{m_a\hat{T}_e^{3/2}}(\hat{T}_e - \hat{T}_g) - \hat{R} \tag{6}$$

where $\mathbf{M}$ is the Righi-Leduc tensor,[10] and where the electron viscosity, but not the electron heat conduction, has been neglected (electron gas Mach number $\ll 1$). It is necessary to include the radiation loss $\hat{R}$ from the electron gas. This term has been obtained separately from the integro-differential equation of radiative transfer.[27,29]

Maxwell's Equations

$$\nabla\cdot(\epsilon_0\hat{\mathbf{E}}) = \hat{\rho}_c \tag{7}$$

$$\nabla \times \hat{\mathbf{E}} = -(\partial\hat{\mathbf{B}}/\partial t) \tag{8}$$

$$\nabla\cdot\hat{\mathbf{B}} = 0 \tag{9}$$

$$\nabla \times (\hat{\mathbf{B}}/\mu_0) = \hat{\mathbf{J}} + [\partial(\epsilon_0\hat{\mathbf{E}})/\partial t] \approx \hat{\mathbf{J}} \tag{10}$$

where the displacement current is negligible for the frequencies considered. [Neglect of the displacement current in Eq. (10) is tantamount to the "quasi-neutral" assumption mentioned earlier, since this equation then implies $\nabla\cdot\hat{\mathbf{J}} = 0$. Equation (7) is then not needed to close the system of equations, but can be used to compute the local charge accumulation, if desired.]

General Dispersion Relation

The MHD generator will be approximated by a channel whose external electrical circuitry and geometric properties affect only the (homogeneous) steady state of the plasma. This is tantamount to assuming $\lambda \ll$ channel dimensions. Although larger λ's may be present, and the steady state is never exactly uniform, the present analysis is expected to indicate the conditions under which actual generators are "potentially" unstable to the modes considered. Although the influence of an inhomogeneous steady state[30] and the electrical and geometric constraints of a generator[5,6] may be important, they are beyond the scope of this paper.

For small perturbations about the (assumed) homogeneous steady state, the preceding set of two-fluid equations can be linearized. A plane wave solution of the form $\hat{A} = A_0 + A\exp[i(\mathbf{k}\cdot\mathbf{x} - \omega t)]$ (where $\mathbf{k}$ is real and transverse to the magnetic field, and $\omega = \omega_r + i\omega_i$) is sought from the equations. Both a small magnetic Reynolds number and slight ionization of the alkali atoms are assumed.

It was found[29] that, although a steady-state radiation loss can be obtained for a finite-size channel, it is necessary to postulate an infinite plasma to obtain the radiation perturbations in terms of a single wave number. It was further found[29] that, for small perturbations, the effect of perturbations of the optical depth per unit length m_ν is negligible compared to that of perturbations of the Planck function B_ν. Under these conditions, the components of the radiation term

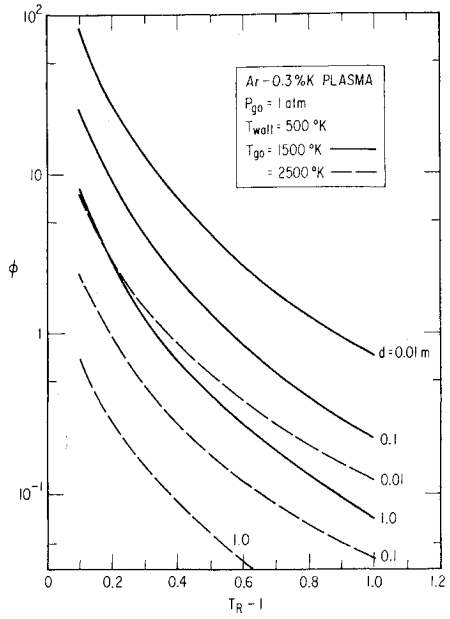

Fig. 1 Ratio ϕ of averaged radiation flux to walls to neutral collisional energy loss vs temperature.

$\hat{R}$ in Eq. (6) are given by[29]

$$R_0 = \tfrac{16}{3}\pi^{3/2}\Delta\nu_0(m_{00}/d)^{1/2}[B_{00}\{T_{e0}\} - B_{00}\{T_{wall}\}] \quad (11)$$

$$R = \frac{4(2)^{1/2}\pi^2}{3} B_{00}m_{00}\Delta\nu_0 \frac{h\nu_0}{KT_{e0}}\left[\frac{|\mathbf{k}|}{m_{00}}\right]^{1/2}\frac{T_e}{T_{e0}} \quad (12)$$

As can be seen from Fig. 1, for an Ar plasma with a low electron temperature elevation, the steady-state radiation loss can be significant in small channels. Because of the large collision cross section of He, the effect of radiation is generally negligible in He-constituted plasmas.

Using the operative transforms $\partial/\partial t \to -i\omega$, $D/Dt \to -i\cdot(\omega - \mathbf{u}_{g0}\cdot\mathbf{k}) \equiv -i\omega'$, and $\nabla \to i\mathbf{k}$, the following equations for the (complex) magnitudes of the plane-wave perturbations are obtained after much manipulation.

Heavy-Gas Momentum Equation

$$\left[iA_{10}\left(\frac{\omega'}{a_0k}\right)^2 + iA_{11}\left(\frac{\omega'}{a_0k}\right) + A_{12}\left(\frac{\omega'}{a_0k}\right) + A_{14}\right]\frac{\rho_g}{\rho_{g0}} + [iB_{13}]\frac{p_g}{p_{g0}} + \left[iC_{11}\left(\frac{\omega'}{a_0k}\right) + C_{14}\right]\frac{n_e}{n_{e0}} = 0 \quad (13)$$

Heavy-Gas Energy Equation

$$\left[iA_{21}\left(\frac{\omega'}{a_0k}\right) + A_{24}\right]\frac{\rho_g}{\rho_{g0}} + \left[iB_{21}\left(\frac{\omega'}{a_0k}\right) + B_{24}\right]\frac{p_g}{p_{g0}} + \left[iC_{21}\left(\frac{\omega'}{a_0k}\right) + C_{24}\right]\frac{n_e}{n_{e0}} = 0 \quad (14)$$

Electron-Gas Energy Equation

$$\left[A_{30}\left(\frac{\omega'}{a_0k}\right)^2 + iA_{31}\left(\frac{\omega'}{a_0k}\right) + A_{32}\left(\frac{\omega'}{a_0k}\right) + iA_{33} + A_{34}\right]\frac{\rho_g}{\rho_{g0}} + [B_{34}]\frac{p_g}{p_{g0}} + \left[C_{30}\left(\frac{\omega'}{a_0k}\right)^2 + iC_{31}\left(\frac{\omega'}{a_0k}\right) + C_{32}\left(\frac{\omega'}{a_0k}\right) + iC_{33} + C_{34}\right]\frac{n_e}{n_{e0}} = 0 \quad (15)$$

All of the coefficients A,B,C, etc. are real and are listed in the Appendix. In Eqs. (13–15), k is the magnitude of the wave vector $\mathbf{k}$. The angle between $\mathbf{k}$ and $\mathbf{J}_0$ is denoted by θ, which appears as a parameter in the coefficients A,B,C, etc. (see Appendix).

Since these equations are homogeneous, for a nontrivial solution to exist the determinant of the coefficients must vanish. Setting this determinant equal to zero gives the dispersion relation, i.e., the relation between ω' and $\mathbf{k}$:

$$\psi_5\left(\frac{\omega'}{a_0k}\right)^5 + \psi_4\left(\frac{\omega'}{a_0k}\right)^4 + \psi_3\left(\frac{\omega'}{a_0k}\right)^3 + \psi_2\left(\frac{\omega'}{a_0k}\right)^2 + \psi_1\left(\frac{\omega'}{a_0k}\right) + \psi_0 = 0 \quad (16)$$

where the ψ's are also defined in the Appendix and depend on θ.

This fifth-order equation with complex coefficients cannot generally be solved analytically. However, computer solutions can be obtained using Muller's[31] quadratic method to locate the roots in the complex plane. The five roots of the equation correspond to four waves: magnetoacoustic (a paired wave), thermal, electrothermal, and "ionization rate."

Wave Limits

Within the limitations of the analysis, the computer solutions give the exact behavior of the waves but show little of the physics. In order to bring out the physical nature of each of the individual modes inherent in Eq (16), simplifying physical assumptions must be made in the set of two-fluid equations; an explicit "simple" solution for the phase velocities and growth rates of each wave is then found. From these, stability criteria, the directions of maximum growth rates, and the general wave characteristics can be obtained[29] and compared with earlier results (see Introduction).

Magnetoacoustic Wave Limit

The dispersion relation for magnetoacoustic (hereafter denoted by "MA") waves can be obtained from Eq. (16) if the following two assumptions are made: 1) the substantial derivative of the electron enthalpy in Eq. (6) is negligible; and 2) the electrons are in instantaneous Saha equilibrium at the electron temperature. The range of validity of these assumptions will be discussed later. Together, they reduce Eq. (16) to a third-order dispersion relation containing the paired MA waves and the thermal ("T") wave. In addition, the following simplifications are made: Coulomb collisions, the

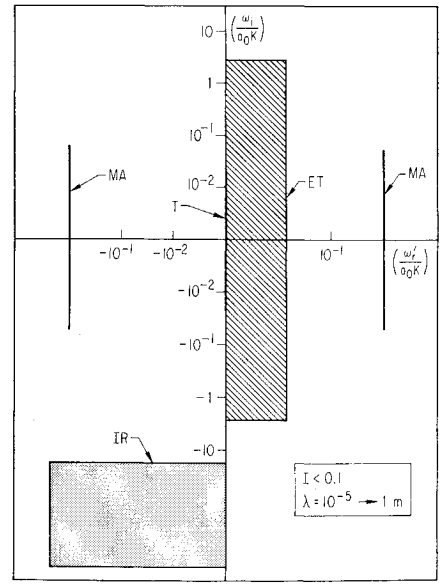

Fig. 2 Locus of the roots of the fifth-order general dispersion relation.

electron pressure gradient, and electron heat convection are assumed negligible, and the momentum collision cross sections are taken to be constant. Assuming $\omega_r'/a_0k \cong 1$ and $\omega_i^2 \ll \omega_r'^2$ (which is equivalent to assuming the interaction parameter, $I = J_0B_0/kp_{g0} \ll 1$), the dispersion relation yields the growth rate[29] for MA waves. For a negligible electron temperature elevation ($T_R = 1$) and no steady-state radiation losses, the equation for the growth rate ω_i simplifies to

$$\omega_i = -\frac{\sigma_0 B_0}{2\rho_{g0}}\left[1 + \frac{u_{e0}}{a_0\beta_0}\left\{\left[(\gamma-1)\frac{\epsilon_i}{2KT_{g0}} + \frac{3\gamma-1}{4}\right]\times \beta_0\cos\theta + \left[(\gamma-1)\frac{\epsilon_i}{2KT_{g0}} - \frac{7\gamma-5}{4}\right]\sin\theta\right\} - (\gamma-1)\left(\frac{u_{e0}}{a_0\beta_0}\right)^2\left\{\left[(\gamma-1)\frac{\epsilon_i}{KT_{g0}} + \frac{3\gamma-1}{2}\right]\times \beta_0\sin\theta\cos\theta + \left[(\gamma-1)\frac{\epsilon_i}{2KT_{g0}} + \frac{\gamma-3}{4}\right]\times (2\sin^2\theta - 1) + (\gamma-1)\frac{(H+R)}{C_{en0}}\right\}\right] \quad (17)$$

As can be seen from Eq. (17), under these circumstances only the normal wave damping, $\sigma_0(\mathbf{u}_g \times \mathbf{B}_0) \times \mathbf{B}_0$ (i.e., the "1") and the heat conduction and radiation terms damp waves in all directions. The effects of all other perturbations, principally those of the electrical conductivity and Hall parameter, can be amplifying for some wave directions. Differentiating Eq. (17) with respect to θ yields the direction of maximum growth, which turns out to be perpendicular to $\mathbf{E}_0'$:

$$\theta_{\max\,\omega_i} \approx \tan^{-1}(1/\beta_0) \quad (18)$$

For large β_0, this direction approaches that of $-\mathbf{J}_0$.

If the foregoing assumption of $T_R = 1$ is relaxed, a qualitatively different ω_i dependence is obtained.[29] With the electron gas no longer completely coupled to the heavy gas, the respective density fluctuations are often completely out of phase. Under these circumstances, not only is the ω_i dependence close to the opposite of that shown in Eq. (17), but the direction of maximum growth rate is essentially opposite to that which single fluid theory has predicted! As it turns out, these circumstances occur whenever electrothermal waves are also unstable.

A stability criterion,[10] based on assuming wave propagation only in the $-\mathbf{J}_0$ direction, predicted that MA waves were always stable for $T_R \gtrsim 1.9$. When the preceding effects are included (i.e., all angles are included), no such completely stable region is found to exist, regardless of the magnitude of T_R.

Thermal Wave Limit

The initial assumptions for the thermal (T) wave limit are identical to those of the MA limit. The T wave corresponds to the third root of the MA-T dispersion relation.[8] We discarded this root previously when we assumed $\omega_r'/a_0k \cong 1$. As the T wave is not present in the absence of dissipation ($\omega' = 0$), we may tentatively assume that $|\omega'/a_0k| \ll 1$ under our conditions of relatively small dissipation. With this assumption, the phase velocity and growth rate for the T wave are obtained.[29] Once again, two-fluid theory gives results essentially the opposite to those predicted by one-fluid theory because of the difference in phase of the electron-gas and heavy-gas density fluctuations.

The phase velocity[29] is of the order of the electron drift velocity times the square of the interaction parameter. Hence, in the absence of a magnetic field, the wave does not propagate. In the presence of a magnetic field, the phase velocity is very small for $J_0B_0/kp_{g0} \ll 1$. However, it can exceed that of the MA wave for $J_0B_0/kp_{g0} > 1$. Furthermore, the T wave is strongly dispersive. The physics of a single root require[3] that ω_r'/k adjust itself to stay within a total range of θ equal to π rad, although this total range need not be made up of adjacent regions.

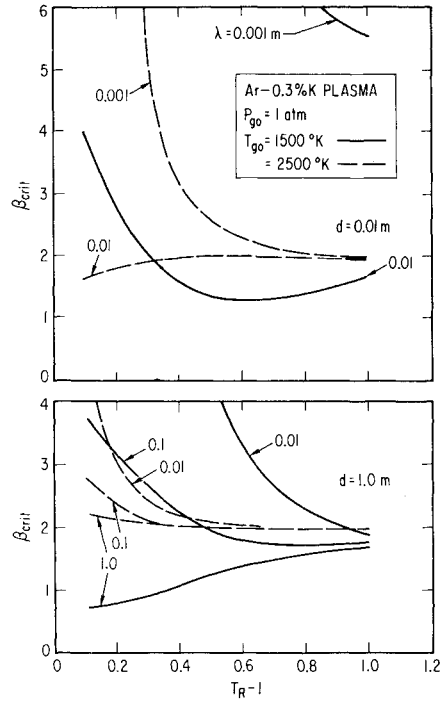

Fig. 3 Critical Hall parameter for electrothermal waves.

The general growth rate equation[29] can be simplified for $T_R = \phi = 0$:

$$\omega_i = \frac{J_0^2/\sigma_0}{(\gamma/\gamma-1)p_{g0}}\left[\left(\frac{\epsilon_i}{KT_{g0}} + \frac{5}{2}\right)\beta_0\sin\theta\cos\theta + \left(\frac{\epsilon_i}{2KT_{g0}} + \frac{3}{4}\right)(2\sin^2\theta - 1) - \frac{(H+R)}{C_{en0}}\right] \quad (19)$$

Thus, the growth rate of T waves is of the order of the ratio of the Joule heating to heavy-gas enthalpy. In fact, all of the terms of Eq. (19) are caused by perturbations in the heavy-gas heating, and, thus, the T-wave instability is purely kinematic. The simplest limit of the T wave is the evanescent root of the ordinary incompressible equation of thermal conduction. However, with the addition of Joule heating, an instability can occur.[12] The limit of Eq. (19) for $H = R = 0$, $\epsilon_i/kT_{g0} \gg 1$, and $\theta = \pi/2$ agrees exactly with the result of Edwards.[3] Because of additional simplifying assumptions made in Ref. 12, the growth rate obtained by Wright is similar but not identical to Eq. (19). Wright[12] assumed incompressibility also. With such an assumption, the heavy-gas momentum equation is uncoupled from the heavy-gas energy equation, and $\omega_r'/k = 0$.

Electrothermal Wave Limit

The additional assumption of the electrothermal ("ET") wave limit over those leading to Eq. (16) is that the heavy gas undergoes no perturbations. This assumption eliminates the two MA roots and T root and leaves a second-order dispersion relation. Furthermore, the assumption turns out to be excellent over a wide regime; ET waves are negligibly dependent on heavy-gas fluctuations[29] for the plasma regime of Fig. 2. For simplicity only, it is assumed in the following that Coulomb collisions are negligible and the momentum collision cross sections are constant. If instantaneous Saha equilibrium were assumed also, the root due to a finite ionization rate ("IR" wave) would be excluded, leaving the single ET root remaining. Although it cannot be justified a priori (Fig. 2), $|\omega'/a_0k|_{ET}$, as it turns out, is much less than $|\omega'/a_0k|_{IR}$. If

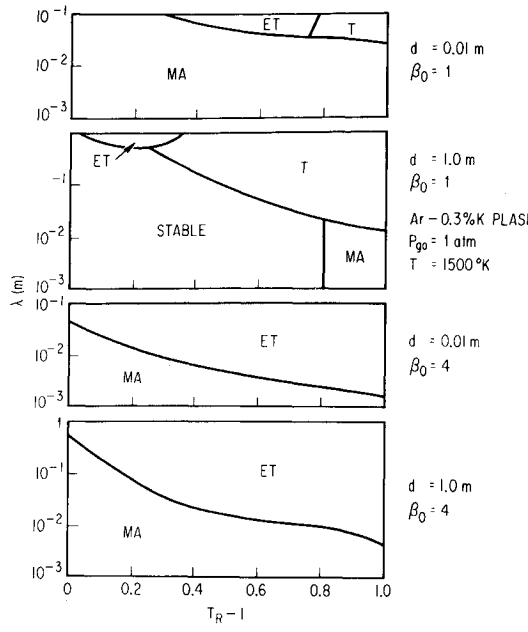

Fig. 4 Dominant mode regimes for an Ar-K plasma.

this result is used, we can avoid the (often very limiting) assumption of instantaneous Saha equilibrium and still obtain simplified but rather general results. The phase velocity and growth rate of the ET mode are then obtained directly,[29] with the effect of finite recombination rate included. In the limit of instantaneous Saha equilibrium, the equation for the ET phase velocity reduces to the result of Kerrebrock,[13]

$$\frac{\omega_r'}{u_{e0}k} = \frac{[(\epsilon_i/\epsilon_{e0}) - \frac{7}{3}]\cos\theta}{2\{1 + \frac{3}{4}[(\epsilon_i/\epsilon_{e0}) - 1]^2\}} \tag{20}$$

Although Eq. (20) indicates a nondispersive wave, a finite recombination rate creates dispersion and reduces the magnitude of the phase velocity. The ET wave propagates in the positive $\mathbf{J}_0$ half-plane, unless the electron temperature is quite high. This is opposite to the electron velocity, because the electron pressure-gradient effects dominate those of heat convection.

In instantaneous Saha equilibrium, the growth rate reduces to

$$\omega_i = \left\langle \frac{\delta m_e}{m_g} \right\rangle \nu_{en0} \left\{ -1 + \left(1 - \frac{T_{g0}}{T_{e0}}\right)\left[-\left(\frac{5}{4} + \frac{\epsilon_i}{2KT_{e0}}\right) + (1+\phi)\left(\frac{1}{4} + \frac{\epsilon_i}{2KT_{e0}}\right)(2\sin^2\theta - 1) + (1+\phi) \times \left(\frac{3}{2} + \frac{\epsilon_i}{KT_{e0}}\right)\beta_0 \sin\theta\cos\theta - \frac{(H+R)}{C_{en0}} \right] \right\} \times \left[1 + \frac{3}{4}\left(\frac{\epsilon_i}{\epsilon_{e0}} - 1\right)^2\right]^{-1} \tag{21}$$

Equation (21) shows that the growth rate for ET wave is of the order of the ratio of the Joule heating to the ionization energy. Unlike the growth rate of MA waves, which is proportional to an interaction parameter and thus is generally small and a very strong function of T_{e0}, the growth rate of ET waves is $O\{10^5\ \text{sec}^{-1}\}$ for Ar and $O\{10^6\ \text{sec}^{-1}\}$ for He and only weakly dependent on T_{e0} (for $k_b \to \infty$). The inclusion of a finite recombination rate[29] reduces ω_i but alters the qualitative aspects little. As long as $k_b n_{e0} \neq 0$, the wave can be unstable. This generalizes the analysis of Kerrebrock,[13] who used a first-order expansion in k_b^{-1} for the effect of a finite recombination rate. He speculated that the extension of this linear expansion might indicate a "critical" $n_{e0} \approx 10^{13}\ \text{cm}^{-3}$ below which ET waves would be always stable. No such stabilization occurs in the more complete theory. Furthermore, with a radiation loss, ET waves not only can exist at a zero electron temperature elevation (provided $J_0^2/\sigma_0 \neq 0$), but can be unstable in such a situation.

Differentiating Eq. (21) with respect to θ gives the direction of maximum growth for ET waves:

$$\theta_{\max \omega_i} = \tfrac{1}{2}\tan^{-1}\{-\beta_0[2r/(2r-1)]\} \approx \tfrac{1}{2}\tan^{-1}(-\beta_0) \tag{22}$$

As β_0 increases, this direction moves away from that of $-\mathbf{J}_0 \times \mathbf{B}_0$ toward that of $+\mathbf{J}_0$. For $\beta_0 \ll 1$, it is equidistant from each of these directions. Waves in the general direction of that given by Eq. (22) are amplified because of the increased local heating given by $\mathbf{J}\cdot\mathbf{E}_0'$ and $\mathbf{J}_0\cdot\mathbf{E}'$ in the regions where n_e is positive.

In general, a magnetic field is required for an ET wave instability. Then, the stability criterion can be put in terms of a critical Hall parameter, β_{crit}. For values of the Hall parameter above β_{crit}, the ET wave is unstable in the direction of maximum amplification. Using Eq. (21) for ω_i, β_{crit} can be calculated and is shown in Fig. 3 as a function of T_R, T_{g0}, d, and λ. For ET waves, radiation and electron heat conduction fluctuations are always damping. Hence, β_{crit} increases as the wavelength decreases. For small wavelengths, β_{crit} is essentially determined by radiation and electron heat conduction damping. For larger values of λ, β_{crit} is governed by collisional losses. A steady-state radiation loss reduces the magnitude of both of these damping effects, thereby increasing the relative amplifying effect of the Joule heating. Results illustrating these trends are shown in Fig. 3. The effects are most dramatic for "small" channels, i.e., for relatively large steady-state radiation losses.

Ionization Rate Wave Limit

The remaining wave contained in the fifth-order dispersion relation is present only with a finite recombination rate. This ionization rate (IR) wave was eliminated from the IR-ET dispersion relation by assuming

$$|\omega'/a_0k|_{\text{ET}} \ll |\omega'/a_0k|_{\text{IR}}$$

If we assume, in contrast, $|\omega'/a_0k| \gg 1$, the dispersion relation yields the IR phase velocity as

$$\omega_r'/u_{e0}k = -\tfrac{5}{3}\cos\theta \tag{23}$$

and the "growth" rate as

$$\omega_i = -\nu_{en0}\left\{2\left[1 + \frac{3}{4}\left(1 + \frac{\epsilon_i}{\epsilon_{e0}}\right)^2\right]\frac{k_b n_{e0}^2}{\nu_{en0}} + \frac{1}{2}\left\langle\frac{\delta m_e}{m_g}\right\rangle\left[(1+\phi)\left(1 - \frac{T_{g0}}{T_{e0}}\right)(2\sin^2\theta - 1) + 3 - \frac{T_{g0}}{T_{e0}}\right] + \frac{2(H+R)}{3KT_{e0}n_{e0}\nu_{en0}}\right\} \tag{24}$$

Equation (23) shows that the IR wave has a high phase velocity, being of the order of u_{e0} and in the same direction. In fact, it is just the rate of heat convection. Equation (24) shows that the IR mode is always damped.

The dominant term in Eq. (24), $-2k_b n_{e0}^2$, is just the reciprocal of the characteristic time it takes to return a displacement of n_e back to the value required by Saha equilibrium. The damping rate is $O\{10^7\text{–}10^8\ \text{sec}^{-1}\}$. The fact that IR waves are strongly damped would not necessarily eliminate them from engineering interest, as they could, in principle, interact with and affect the behavior of the MA, T, or ET waves. However, we see below that any linear interaction is negligible, and thus the IR wave is in fact unimportant.

Low R_{em}, MHD Waves

The foregoing approximate treatments of the various modes brings out some of the physics of MHD waves and establishes

contact with earlier work. Unfortunately, the physical insight thus gained comes at the expense of several limiting approximations (whose range of validity is not easy to establish) and also the elimination of any consideration of possible linear coupling between the various waves. Since such interactions, as well as the limiting approximations, could significantly affect the behavior of the individual waves, the roots of the full dispersion relation, Eq. (16), will now be discussed. Figure 2 shows the locus of these roots for typical conditions.

Because of the wide separation in the complex plane of the roots, it is possible, using appropriate *mathematical* approximations, to obtain explicit expressions for ω_i and ω_r' for all of the waves individually. These expressions,[29] which we refer to as the "distinct" wave theories, give generally better approximations for the growth rates and frequencies than do those of the previous "simple" wave limits. In fact, as we shall see below, for MA waves with $\lambda \lesssim 0.1$ m, the "distinct" MA wave theory is the only valid (approximate) MA theory. Because each "distinct" wave theory in effect assumes the existence of only a single wave type, the resulting growth rate and frequency can be compared to the corresponding exact root of the fifth-order dispersion relation to determine the presence of any linear wave coupling. Such a comparison has been carried out in Ref. 29; no evidence of linear wave coupling was found throughout the regime indicated in Fig. 2. However, with a higher interaction parameter in an He-Cs plasma, ET and T waves can couple. Nevertheless, their growth rates are still substantially those predicted by the "distinct" wave theories. Whenever linear interaction of the modes is negligible, the properties of the modes given by the "distinct" wave theories[29] are virtually identical to those obtained from numerical solution of the full dispersion relation.

From the roots of Eq. (16), the most unstable mode can be determined for given plasma conditions. The plasma regimes for which a particular wave mode "dominates" (i.e., has the largest growth rate) are shown in Fig. 4. As can be seen, at least on the basis of this criterion, magnetoacoustic waves tend to dominate at small wavelengths, particularly at small-to-moderate Hall parameters, whereas for large β_0 and significant electron temperature elevation, electrothermal waves become the most important, as expected. Note that there are also regimes for which the thermal mode is "dominant." It should be noted, however, that, whenever the ET waves are dominant, they tend to have dramatically higher growth rates than the maximum attained by the other modes.

The exact numerical results for various wave modes will now be discussed in more detail, beginning with the MA mode.

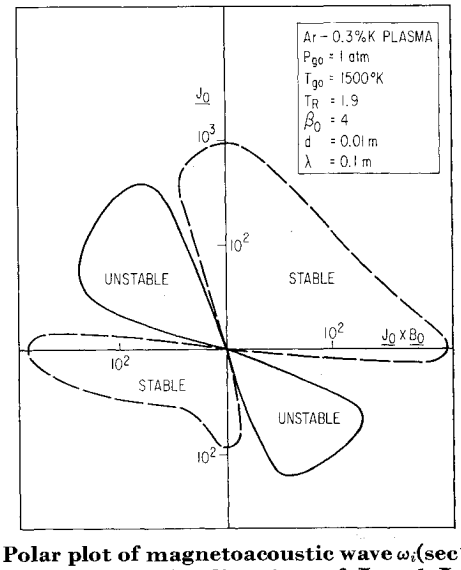

Fig. 5 Polar plot of magnetoacoustic wave ω_i(sec^{-1}). The reference axes are in the directions of $\mathbf{J}_0$ and $\mathbf{J}_0 \times \mathbf{B}_0$, as labeled. See text for explanation of high λ/d ratio.

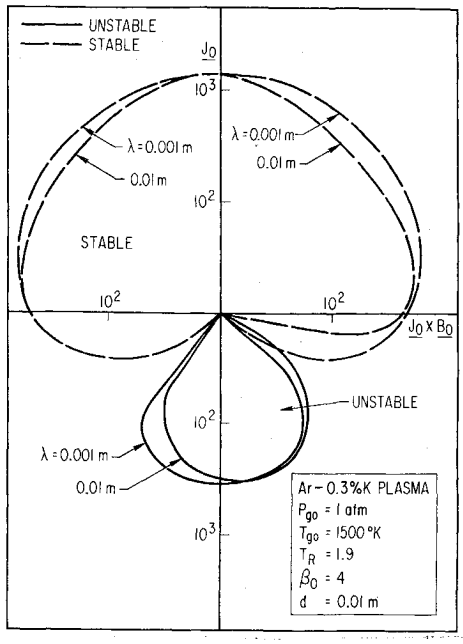

Fig. 6 Polar plot of magnetoacoustic wave ω_i(sec^{-1}).

Figure 5 is a polar plot of $\omega_{i_{MA}}$ for a long (0.1 m) wavelength at conditions relevant to the "simple" two-fluid MA theory. It is plotted here for $d = 0.01$ m only to allow direct comparison with Fig. 6; for $T_R = 1.9$, the value of d has little effect on the waves, so that in fact Fig. 5 is little altered if one chooses $d = 1.0$ m. (Figures 5, 6, 8, and 9 are plotted on a logarithmic scale, for which the graph region for small values of ω_i has been condensed to a point at the origin.) Figure 5 agrees well with the "simple" two-fluid theory, except for the fact that Coulomb collisions, included in the calculations shown in this plot, have stabilized the wave in the $-\mathbf{J}_0$ direction and increased ω_i in the unstable regions. In the absence of Coulomb collisions, the wave in the $-\mathbf{J}_0$ direction would be unstable. Single-fluid theory would predict only a small region around the $-\mathbf{J}_0$ direction to be unstable.

A very striking qualitative difference in the behavior of ω_i between Figs. 5 and 6 is evident, although the only difference is the smaller wavelengths used in obtaining Fig. 6. Chiefly it is the effect of the rate of change of electron enthalpy that has shifted the ω_i behavior so drastically. If this were not taken into account [e.g., if the "simple" (two-fluid) theory were used], the plot of ω_i would be very similar to Fig. 5 and

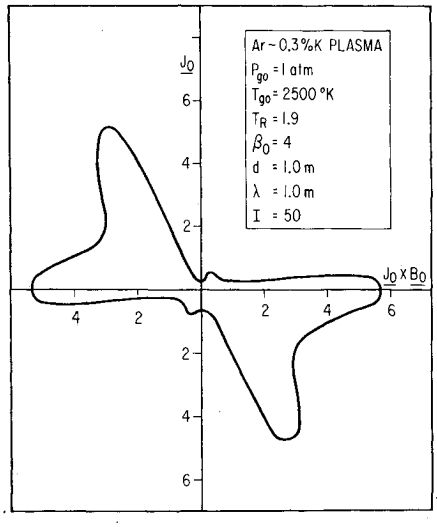

Fig. 7 Polar plot of magnetoacoustic wave phase velocity ω_r'/a_0k.

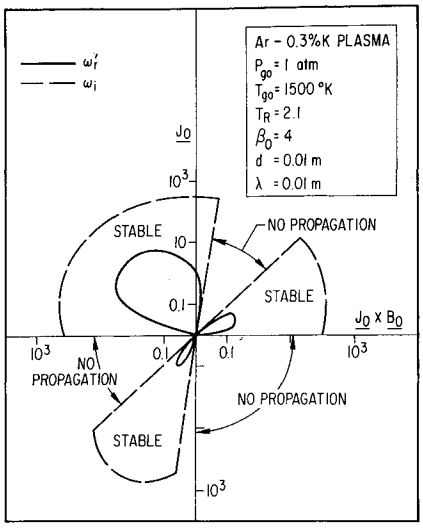

Fig. 8 Polar plot of thermal wave ω_r' and ω_i(sec^{-1}).

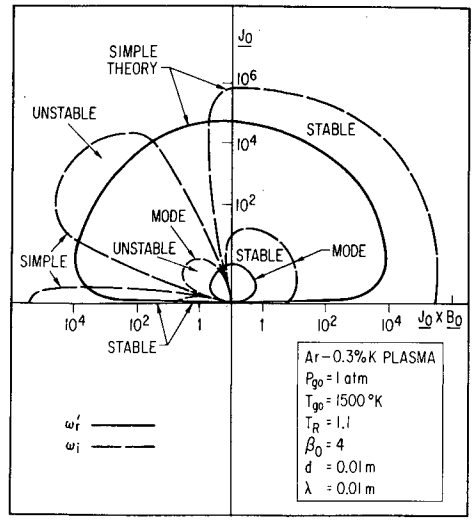

Fig. 9 Polar plot of electrothermal wave ω_r' and ω_i(sec^{-1}). The curves labeled "mode" were obtained from the "distinct" electrothermal wave theory, described in the text, and include the effects of finite recombination rate.

quite incorrect. It should be stressed that, although Fig. 6 is qualitatively similar to what the simple one-fluid theory would predict, this is strictly fortuitous. The physics of the MA modes in this regime is quite different from that of the simple one-fluid model.

As was seen in Fig. 2, for $I < 0.1$ the phase velocity of the MA wave is negligibly affected by perturbations in the **E** (and **B**) fields and simply equals the isentropic speed of sound. However, for $I > 0.1$, it becomes more and more strongly influenced by these fields. An example is illustrated in Fig. 7. To be strictly valid, Fig. 7 would have to be modified to include finite R_{em}, which goes beyond the scope of our present treatment. An extension of the theory along the lines of Ref. 3, but including two-fluid effects, is required to obtain accurate results at such high interaction parameters. In any case, however, strong departures of the phase speed of the MA wave from the gas sound speed are expected, and Fig. 7 shows that these can occur even in the absence of perturbations in **B**.

Figure 8 shows some characteristics of the T wave. The T wave is damped for $T_R \lesssim 2.0$ if $\lambda = 0.01$ m and $\beta_0 = 4$. For $\lambda = 0.1$ m and $\beta_0 = 4$, the stability criterion drops to $T_R \lesssim 1.6$. Thus, the thermal wave is much more stable than Wright[12] or Powers and Dicks[8] predicted. This is because of the large damping due to radiation and heat conduction fluctuations and because a two-fluid model is absolutely necessary to give the correct ω_i if a temperature elevation is present.

Figure 9 shows the typical ET wave behavior. The phase velocity is approximately a cosine curve in the $+\mathbf{J}_0$ half-plane, whereas the wave is unstable in a portion of the second quadrant. However, Fig. 9 shows the tremendous quantitative difference (over four orders of magnitude!) at this temperature between the actual ET mode and the result of the simplified ET theory, which neglects the effect of a finite recombination rate. The results of the full theory agree within 0.1% with the results of the "distinct" wave theory for this mode, and it is the latter set of results which is labeled "mode" in Fig. 9. At higher electron temperatures, the error inherent in the simplified theory is less, but it is still observable below $T_{e0} = 3000$°K.

It is because of the appropriateness to some experiments that $d = 0.01$ m has been taken for Figs. 5, 6, 8, and 9. It should be emphasized that every qualitative effect shown in Figs. 5–9 is present under conditions of strict validity of the theory ($\lambda \ll d$). That is, no new (qualitative) effects have appeared simply because we have "stretched" our results to the limit $\lambda \approx d$ in making the preceding plots. That this is so has been checked through much more extensive calculations, results of which are available in Ref. 29.

Experiments

The present linear analysis cannot, of course, give the fluctuation amplitudes or the reduction in effective β_0 and σ_0, which are often the only applicable parameters experimentally determined. To obtain these, a nonlinear theory, c.f. Solbès,[16] is required. However, several experiments have recorded data to which the present analysis can be directly compared.

Belousov et al.[19] measured ω_r'/k and θ in a medium-pressure Ar-Cs pulse discharge without gas flow. For $\beta_0 = 0$, the plasma was homogeneous. For $\beta_0 = 1$, $\theta_{meas} = 65°$ (vs 67.5° from ET theory), and for $\beta_0 = 3$, $\theta_{meas} = 57°$ (vs 54°). The phase velocity (1.5×10^3 cm/sec) and growth rate were also in agreement with ET theory.

Lopatsky and Andropov,[20] in a similar discharge experiment, found instabilities for $\beta_0 = 1$. Both MA and ET waves were theoretically unstable. Phase velocities and wavelengths were measured but unfortunately not included in Ref. 20.

Brederlow and Hodgson[21] measured ω_r'/k and θ in a high-pressure Ar-K discharge. For $\beta_0 \leq 2$, waves antiparallel to $\mathbf{J}_0$ with $\omega_r'/k = 50$ m/sec were found. This does not agree with either MA or ET wave theory predictions. Further measurements showed that 1) for $\beta_0 = 2.2$, $\theta = 55°$ (vs 57° from ET theory), and $\omega_r'/k = 30$ m/sec (vs 19 m/sec); and 2) for $\beta_0 = 3.3$, $\theta = 54°$ (vs 53°), and $\omega_r'/k = 33$ m/sec (vs 19 m/sec). When ω_r'/k is calculated from an ET theory that includes a finite k_b, the agreement is much better. Riedmüller,[26] using the same apparatus, found $\beta_{crit} \simeq 1$, which is in general agreement with Fig. 3 for his parameter values.

In a similar type of discharge, Kerrebrock and Dethlefsen[22] found sharply increasing fluctuation magnitudes at $\beta_0 > \beta_{crit}$ (c.f. Fig. 3). The characteristics of these instabilities agree well with ET theory predictions. For $\beta_0 < \beta_{crit}$, smaller fluctuations were observed where MA waves should be unstable. However, the residence time in the channel for a propagating MA wave is small compared to ω_{iMA}, implying that if these fluctuations are due to MA waves they must be essentially "standing" in the channel. This situation is possible for MA modes, in contrast to the remaining modes, because the MA waves occur in pairs.

Conclusions

The present analysis has sought to provide a greater understanding of low-R_{em} MHD waves by making as few limiting assumptions as possible and then determining the individual wave characteristics and the interrelationship of these waves. Important differences in wave characteristics from those of previous theories have been discovered. Furthermore, linear wave coupling was found to be negligible in most regimes of interest, so that "distinct" wave analyses are useful. The physics of all three of the unstable waves has one striking common feature, viz., the phase difference between the electron-gas and heavy-gas density fluctuations; the stability boundary for ET waves is identical to the boundary between one-fluid and two-fluid "behavior" for MA waves, and this is in turn identical to the condition for nonexistence of T waves.

Appendix

The coefficients for Eqs. (13–15) are

$$A_{10} = -\gamma$$

$$A_{11} = I(a_0k/2k_bn_{e0}^2)(S_1/r)\sin\theta$$

$$A_{12} = I(a_0\beta_0/u_{e0})$$

$$A_{14} = IS_3\sin\theta$$

$$B_{13} = 1$$

$$C_{11} = I(a_0k/2k_bn_{e0}^2)(S_1/r)\sin\theta$$

$$C_{14} = I(\beta_0\cos\theta + S_2\sin\theta)$$

$$A_{21} = \frac{2\gamma}{3(\gamma-1)}\left\langle\delta\frac{m_e}{m_g}\right\rangle^{-1}\frac{n_{g0}}{n_{e0}}\frac{a_0k}{\nu_{en0}} - \frac{1}{2r}\frac{a_0k}{k_bn_{e0}^2}\times\left\{\left(\frac{1}{2}+\varphi\right)(T_R-1)+T_R+C_r\left[\left(\frac{3}{2\ln\Lambda_0}-\frac{3}{2}\right)(T_R-1)+T_R\right]\right\}$$

$$A_{24} = -C_r - T_R + \frac{1}{2r}\left\{\left(\frac{1}{2}+\varphi\right)(T_R-1)+T_R+C_r\left[\left(\frac{3}{2\ln\Lambda_0}-\frac{3}{2}\right)(T_R-1)+T_R\right]\right\}$$

$$B_{21} = -\frac{2}{3(\gamma-1)}\left\langle\delta\frac{m_e}{m_g}\right\rangle^{-1}\frac{n_{g0}}{n_{e0}}\frac{a_0k}{\nu_{en0}}$$

$$B_{24} = 1 + C_r$$

$$C_{21} = \frac{1}{2r}\frac{a_0k}{k_bn_{e0}^2}\left\{\left(\frac{1}{2}+\varphi\right)(T_R-1)+T_R+C_r\left[\left(\frac{3}{2\ln\Lambda_0}-\frac{3}{2}\right)(T_R-1)+T_R\right]\right\}$$

$$C_{24} = 1 - T_R + C_r\left(\frac{1}{2\ln\Lambda_0}-2\right)(T_R-1) - \frac{1}{r}\left\{\left(\frac{1}{2}+\varphi\right)(T_R-1)+T_R+C_r\left[\left(\frac{3}{2\ln\Lambda_0}-\frac{3}{2}\right)(T_R-1)+T_R\right]\right\}$$

$$A_{30} = \frac{1}{2r}\frac{T_R}{T_R-1}\frac{a_0k}{k_bn_{e0}^2}\left\langle\delta\frac{m_e}{m_g}\right\rangle^{-1}\frac{a_0k}{\nu_{en0}}$$

$$A_{31} = \frac{[5+(3/2r)]T_R+2(\epsilon_i/kT_{g0})}{3(T_R-1)}\left\langle\delta\frac{m_e}{m_g}\right\rangle^{-1}\frac{a_0k}{\nu_{en0}} + \frac{1}{r}\frac{a_0k}{2k_bn_{e0}^2}\left[\frac{1}{2}+\varphi+C_r\left(\frac{3}{2\ln\Lambda_0}-\frac{3}{2}\right)+\frac{(1+C_r)T_R}{T_R-1}+(1+C_r+\phi)S_1(2\sin^2\theta-1)+\frac{(H+R)}{C_{en0}}\right]$$

$$A_{32} = (1+C_r+\phi)\left(-2\frac{a_0}{u_{e0}}\beta_0\sin\theta + \frac{5\pi}{32r}\frac{a_0k}{k_bn_{e0}^2}\frac{\langle v_{e0}\rangle}{u_{e0}}\frac{\langle v_{e0}\rangle k}{\nu_{t0}}\cos\theta\right)$$

$$A_{33} = (1+C_r+\phi)\frac{5\pi}{32r}\frac{\langle v_{e0}\rangle}{u_{e0}}\frac{\langle v_{e0}\rangle k}{\nu_{t0}}\cos\theta$$

$$A_{34} = 1 - \frac{1}{4r} - \frac{\varphi}{2r} - \frac{C_r}{2r}\left(\frac{3}{2\ln\Lambda_0}-\frac{3}{2}\right) + \frac{(1+C_r)[1-(1/2r)T_R]}{(T_R-1)} - (1+C_r+\phi)S_3\times(2\sin^2\theta-1) - \frac{1}{2r}\frac{(H+R)}{C_{en0}}$$

$$B_{34} = -(1+C_r)/(T_R-1)$$

$$C_{30} = -\frac{1}{2r}\frac{T_R}{(T_R-1)}\frac{a_0k}{k_bn_{e0}^2}\left\langle\delta\frac{m_e}{m_g}\right\rangle^{-1}\frac{a_0k}{\nu_{en0}}$$

$$C_{31} = -\frac{[3+(3/r)]T_R+2(\epsilon_i/kT_{g0})}{3(T_R-1)}\left\langle\delta\frac{m_e}{m_g}\right\rangle^{-1}\frac{a_0k}{\nu_{en0}} - \frac{1}{r}\frac{a_0k}{2k_bn_{e0}^2}\left[\frac{1}{2}+\varphi+C_r\left(\frac{3}{2\ln\Lambda_0}-\frac{3}{2}\right)+\frac{(1+C_r)T_R}{T_R-1}+(1+C_r+\phi)S_1(2\sin^2\theta-1)+\frac{(H+R)}{C_{en0}}\right]$$

$$C_{32} = -(1+C_r+\phi)\frac{5\pi}{32r}\frac{a_0k}{k_bn_{e0}^2}\frac{\langle v_{e0}\rangle}{u_{e0}}\frac{\langle v_{e0}\rangle k}{\nu_{t0}}\cos\theta$$

$$C_{33} = (1+C_r+\phi)\left(\frac{\pi}{8}-\frac{5\pi}{16r}\right)\frac{\langle v_{e0}\rangle}{u_{e0}}\frac{\langle v_{e0}\rangle k}{\nu_{t0}}\cos\theta$$

$$C_{34} = 1 + \frac{1}{2r} + \frac{\varphi}{r} + C_r\left[\left(\frac{3}{r}-1\right)\frac{1}{2\ln\Lambda_0}-\frac{3}{2r}+2\right] + \frac{1}{r}\frac{(1+C_r)T_R}{(T_R-1)} - (1+C_r+\phi)2\beta_0\sin\theta\cos\theta - (1+C_r+\phi)S_2(2\sin^2\theta-1) + \frac{(H+R)}{C_{en0}}$$

where φ, S_1, S_2, and S_3 account for variable collision cross sections and are $O\{1\}$; c.f. Eqs. (2.12) and (9.10) of Ref. 29.

The ψ's of Eq. (16) defined in terms of the preceding coefficients are

$$\psi_5 = (-A_{10}B_{21}C_{30})$$

$$\psi_4 = (-A_{10}B_{21}C_{32} - A_{11}B_{21}C_{30} + A_{30}B_{21}C_{11}) + i(-A_{10}B_{21}C_{31} + A_{12}B_{21}C_{30} + A_{10}B_{24}C_{30})$$

$$\psi_3 = (-A_{10}B_{21}C_{34} - A_{11}B_{21}C_{32} - A_{12}B_{21}C_{31} - A_{10}B_{24}C_{31} + A_{12}B_{24}C_{30} + A_{10}B_{34}C_{21} + A_{21}B_{13}C_{30} - A_{30}B_{13}C_{21} + A_{32}B_{21}C_{11}) + i(-A_{10}B_{21}C_{33} - A_{11}B_{21}C_{31} + A_{12}B_{21}C_{32} + A_{14}B_{21}C_{30} + A_{10}B_{24}C_{32} + A_{11}B_{24}C_{30} - A_{30}B_{21}C_{14} - A_{30}B_{24}C_{11} + A_{31}B_{21}C_{11})$$

$$\psi_2 = (-A_{11}B_{21}C_{34} - A_{12}B_{21}C_{33} - A_{14}B_{21}C_{31} - A_{10}B_{24}C_{33} - A_{11}B_{24}C_{31} + A_{12}B_{24}C_{32} + A_{14}B_{24}C_{30} + A_{11}B_{34}C_{21} + A_{21}B_{13}C_{32} - A_{21}B_{34}C_{11} - A_{32}B_{13}C_{21} - A_{30}B_{24}C_{14} + A_{31}B_{21}C_{14} + A_{31}B_{24}C_{11} + A_{34}B_{21}C_{11}) + i(-A_{11}B_{21}C_{33} + A_{12}B_{21}C_{34} + A_{14}B_{21}C_{32} + A_{10}B_{24}C_{34} + A_{11}B_{24}C_{32} + A_{12}B_{24}C_{31} - A_{12}B_{34}C_{21} - A_{10}B_{34}C_{24} + A_{21}B_{13}C_{31} - A_{24}B_{13}C_{30} - A_{31}B_{13}C_{21} + A_{30}B_{13}C_{24} - A_{32}B_{21}C_{14} - A_{32}B_{24}C_{11} + A_{33}B_{21}C_{11})$$

$$\psi_1 = (-A_{14}B_{21}C_{33} - A_{11}B_{24}C_{33} + A_{12}B_{24}C_{34} + A_{14}B_{24}C_{32} - A_{12}B_{34}C_{24} + A_{21}B_{13}C_{34} + A_{24}B_{13}C_{31} - A_{34}B_{13}C_{21} - A_{31}B_{13}C_{24} - A_{32}B_{24}C_{14} + A_{33}B_{21}C_{14} + A_{33}B_{24}C_{11}) + i(+A_{14}B_{21}C_{34} + A_{11}B_{24}C_{34} + A_{12}B_{24}C_{33} + A_{14}B_{24}C_{31} - A_{14}B_{34}C_{21} - A_{11}B_{34}C_{24} + A_{21}B_{13}C_{33} - A_{24}B_{13}C_{32} + A_{21}B_{34}C_{14} + A_{24}B_{34}C_{11} - A_{33}B_{13}C_{21} + A_{32}B_{13}C_{24} - A_{31}B_{24}C_{14} - A_{34}B_{21}C_{14} - A_{34}B_{24}C_{11})$$

$$\psi_0 = (+A_{14}B_{24}C_{34} - A_{14}B_{34}C_{24} + A_{24}B_{13}C_{33} + A_{24}B_{34}C_{14} - A_{33}B_{13}C_{24} - A_{34}B_{24}C_{14}) + i(+A_{14}B_{24}C_{33} - A_{24}B_{13}C_{34} + A_{34}B_{13}C_{24} - A_{33}B_{24}C_{14})$$

References

[1] Herlofson, N., "Magneto-hydrodynamic Waves in a Compressible Fluid Conductor," *Nature*, Vol. 165, No. 4208, June 1950, pp. 1020–1021.

[2] Velikhov, E. P., "Hall Instability of a Current Carrying Slightly Ionized Plasma," *Proceedings Symposium on Magnetoplasmadynamic Electrical Power Generation*, 1962, Newcastle-upon-Tyne, England, pp. 135–136.

[3] Edwards, K. R., "Magnetohydrodynamic Wave Propagation in a Partially Ionized Current-Carrying Gas," Ph.D. thesis, Aug. 1967, Dept. of Electrical Engineering, MIT, Cambridge, Mass.

[4] McCune, J. E., "Wave Growth and Instability in Partially Ionized Gases," *Proceedings, Symposium on MHD Electrical Power Generation*, 1964, Paris, pp. 523–538.

[5] Fishman, F. J., "Instability of Hall MHD Generators to Magneto-Acoustic Waves," RR 323, Feb. 1969, Avco Everett Research Lab., Everett, Mass.

[6] McCune, J. E., "Linear Theory of an MHD Oscillator," *Advanced Energy Conversion*, Vol. 5, No. 3, Nov. 1965, pp. 221–240.

[7] Locke, E. V. and McCune, J. E., "Growth Rates for Axial Magneto-Acoustic Waves in a Hall Generator," *AIAA Journal*, Vol. 4, No. 10, Oct. 1966, pp. 1748–1751.

[8] Powers, W. and Dicks, J. B., Jr., "Transient Wave Growth in Magnetogasdynamic Generators," *The Eighth Symposium of Engineering Aspects of Magnetohydrodynamics*, March 1967, Stanford, Calif.

[9] Messerle, H. K., "Traveling Wave Interaction and Wave Growth in a Dense Plasma," *The Physics of Fluids*, Vol. 8, No. 11, Nov. 1965, pp. 1995–2005.

[10] Hollweg, J. V., "Acoustic and Electrothermal Hall Instabilities in Gases," S.M. thesis, June 1965, MIT, Cambridge, Mass.

[11] Eliseev, B. V., "Instability of the Ponderomotive Force in a Weakly Ionized Plasma," *High Temperature*, Vol. 2, No. 6, Nov.–Dec. 1964, pp. 767–773.

[12] Wright, J. K., "A Temperature Instability in Magnetohydrodynamic Flow," *Proceedings of the Physical Society*, Vol. 81, No. 521, March 1963, pp. 498–505.

[13] Kerrebrock, J. L., "Nonequilibrium Ionization Due to Electron Heating, Part I: Theory," *AIAA Journal*, Vol. 2, No. 6, June 1964, pp. 1072–1080.

[14] Velikhov, E. P. and Dykhne, A. M., "Plasma Turbulence Due to the Ionization Instability in a Strong Magnetic Field," *Sixth International Conference on Ionization Phenomena in Gases*, 1963, Paris.

[15] Nelson, A. H. and Haines, M. G., "Analysis of the Nature and Growth of Electrothermal Waves," *Plasma Physics*, Vol. 11, No. 10, Oct. 1969, pp. 811–837.

[16] Solbès, A., "Nonlinear Plane Wave Study of Electrothermal Instabilities in Non-equilibrium Plasmas," *The Eighth Symposium on Engineering Aspects of Magnetohydrodynamics*, March 1967, Stanford, Calif.

[17] Zampaglione, V., "Effect of an Electron Current along the Magnetic Field on the Development of Ionization Instability in a Low Temperature Plasma," *Plasma Physics*, Vol. 12, No. 1, Jan. 1970, pp. 23–30.

[18] Smith, J. M., "Electrothermal Instabilities in the Entrance Region of an MHD Generator," TM X-1761, March 1969, NASA.

[19] Belousov, V. N., Yeliseyev, V. V., and Shipuk, I. Ya., "Ionization Instability and Turbulent Conductivity of a Non-equilibrium Plasma," *Proceedings, International Symposium on MHD Electrical Power Generation*, 1966, Salzburg, Vol. 2, pp. 323–334.

[20] Lopatsky, G. S. and Andropov, V. G., "Experimental Investigation of the Characteristics of an Arc Discharge in a Transverse Magnetic Field," *Proceedings, International Symposium on MHD Electrical Power Generation*, 1966, Salzburg, Vol. 2, pp. 133–139.

[21] Brederlow, G. and Hodgson, R. T., "Electrical Conductivity in Seeded Noble Gas Plasmas in Crossed Electric and Magnetic Fields," *AIAA Journal*, Vol. 6, No. 7, July 1968, pp. 1277–1284.

[22] Kerrebrock, J. L. and Dethlefsen, R., "Experimental Investigation of Fluctuations in a Nonequilibrium MHD Plasma," *AIAA Journal*, Vol. 6, No. 11, Nov. 1968, pp. 2115–2121.

[23] Nedospasov, A. V. and Shipuk, I. Ya., "Study of Plasma Conductivity in a Transverse Magnetic Field," *High Temperature*, Vol. 3, No. 2, March–April 1965, pp. 166–170.

[24] Zukoski, E. E. and Gilpin, R. R., "Large Amplitude Electrothermal Waves in a Non-equilibrium Plasma," *The Eighth Symposium on Engineering Aspects of Magnetohydrodynamics*, March 1967, Stanford, Calif.

[25] Dicks, J. B. et al., "Characteristics of a Family of Diagonal Conducting Wall MHD Generators," *The Eighth Symposium on Engineering Aspects of Magnetohydrodynamics*, March 1967, Stanford, Calif.

[26] Riedmüller, W., "Experimental Investigation of Instabilities in a Potassium-Seeded Argon Plasma in Crossed Electric and Magnetic Fields," *Proceedings, International Symposium on MHD Power Generation*, 1968, Warsaw, pp. 519–528.

[27] Lutz, M. A., "Radiation and its Effect on the Non-equilibrium Properties of a Seeded Plasma," Ph.D. thesis, Sept. 1965, Dept. of Aeronautics and Astronautics, MIT, Cambridge, Mass.

[28] BenDaniel, D. J. and Tamor, S., "Non-equilibrium Ionization in Magnetohydrodynamic Generators," 62-RL-(2922E), Jan. 1962, General Electric Research Lab., Schenectady, N.Y.

[29] Hougen, M. L., "Magnetohydrodynamic Waves in a Weakly Ionized, Radiating Plasma," Ph.D. thesis, June 1968, Dept. of Aeronautics and Astronautics, MIT, Cambridge, Mass.

[30] Zampaglione, V., "Influence of Plasma Non-homogeneities on the Magneto-acoustic Instabilities," *Proceedings, International Symposium on MHD Power Generation*, 1968, Warsaw, pp. 583–592.

[31] Muller, D. E., "A Method for Solving Algebraic Equations using an Automatic Computer," *Mathematical Tables and Other Aids to Computation*, Vol. 10, No. 4, Oct. 1956, pp. 208–215.